Minimally Manipulated Bone Marrow Concentrate Compared with Microfracture Treatment of Full-Thickness Chondral Defects

A One-Year Study in an Equine Model

Constance R. Chu, MD, Lisa A. Fortier, DVM, PhD, Ashley Williams, MS, Karin A. Payne, PhD, Taralyn M. McCarrel, DVM, Megan E. Bowers, PhD, and Diego Jaramillo, MD, MPH

Investigation performed at the College of Veterinary Medicine, Cornell University, Ithaca, New York; the Department of Orthopedic Surgery at the University of Pittsburgh, Pittsburgh, Pennsylvania and at Stanford University, Stanford, California; and the Departments of Orthopedic Surgery and Radiology, VA Palo Alto Health Care System, Palo Alto, California

Background: Microfracture is commonly performed for cartilage repair but usually results in fibrocartilage. Microfracture augmented by autologous bone marrow concentrate (BMC) was previously shown to yield structurally superior cartilage repairs in an equine model compared with microfracture alone. The current study was performed to test the hypothesis that autologous BMC without concomitant microfracture improves cartilage repair compared with microfracture alone.

Methods: Autologous sternal bone marrow aspirate (BMA) was concentrated using a commercial system. Cells from BMC were evaluated for chondrogenic potential in vitro and in vivo. Bilateral full-thickness chondral defects (15-mm diameter) were created on the midlateral trochlear ridge in 8 horses. Paired defects were randomly assigned to treatment with BMC without concomitant microfracture, or to microfracture alone. The repairs were evaluated at 1 year by in vitro assessment, arthroscopy, morphological magnetic resonance imaging (MRI), quantitative T2-weighted and ultrashort echo time enhanced T2* (UTE-T2*) MRI mapping, and histological assessment.

Results: Culture-expanded but not freshly isolated cells from BMA and BMC underwent cartilage differentiation in vitro. In vivo, cartilage repairs in both groups were fibrous to fibrocartilaginous at 1 year of follow-up, with no differences observed between BMC and microfracture by arthroscopy, T2 and UTE-T2* MRI values, and histological assessment ($p > 0.05$). Morphological MRI showed subchondral bone changes not observed by arthroscopy and improved overall outcomes for the BMC repairs ($p = 0.03$). Differences in repair tissue UTE-T2* texture features were observed between the treatment groups ($p < 0.05$).

Conclusions: When BMC was applied directly to critical-sized, full-thickness chondral defects in an equine model, the cartilage repair results were similar to those of microfracture. Our data suggest that, given the few mesenchymal stem cells in minimally manipulated BMC, other mechanisms such as paracrine, anti-inflammatory, or immunomodulatory effects may have been responsible for tissue regeneration in a previous study in which BMC was applied to microfractured repairs. While our conclusions are limited by small numbers, the better MRI outcomes for the BMC repairs may have been related to reduced surgical trauma to the subchondral bone.

Clinical Relevance: MRI provides important information on chondral defect subsurface repair organization and subchondral bone structure that is not well assessed by arthroscopy.

Chondral injuries contribute to progressive articular cartilage loss and the eventual development of osteoarthritis[1-3], a major public health issue[4,5]. Articular cartilage has limited capacity to repair lesions that do not extend into the underlying bone[6,7]. Strategies to improve cartilage repair are therefore important in the effort to reduce the disease burden of osteoarthritis.

Disclosure: This study was funded by the National Institutes of Health RC2 AR058929 (C.R.C., L.A.F.), R01 AR 051963 (C.R.C.), and R01 AR 052784 (C.R.C.). The funding agency played no role in the investigation. The **Disclosure of Potential Conflicts of Interest** forms are provided with the online version of the article (http://links.lww.com/JBJS/E543).

Microfracture is widely used to access bone marrow cells for cartilage repair[8,9]. While considered a clinical standard[10,11], microfracture has variable clinical outcomes[12-15]. Among professional athletes, results after microfracture range from the resumption of high-performance sports to continued disability[16-19]. Variability in the amount and quality of cartilage-repair tissues, along with the observation of subchondral bone changes after microfracture, has also been reported[15,20-22]. Recently, surgical compromise of the subchondral bone has been postulated to negatively affect subsequent treatment with other cartilage-repair techniques[14,15,20,21].

The amount and quality of repair cells available to the cartilage wound also remain key variables in the success or failure of bone marrow cell-based cartilage repair. Marrow stimulation accesses local bone marrow cells[7,8,21]. Bone marrow aspirate (BMA) can be obtained from sites with higher concentrations of mesenchymal cells, such as the iliac crest in humans or the sternum in an equine model, and centrifuged at the point of care to concentrate potential reparative cells[23,24]. Human clinical studies have shown that autologous bone marrow concentrate (BMC) suspended in collagen or hyaluronic acid scaffolds supports repair of full-thickness chondral defects[25-27]. Prior work in an equine model showed that augmentation of microfracture with BMC resulted in structurally and biochemically improved cartilage repair compared with microfracture alone[23]. To address concerns about potential undesired subchondral bone changes after microfracture, we performed the current study to test the hypothesis that arthroscopically applied BMC without concomitant microfracture improves full-thickness chondral defect repair compared with microfracture alone.

Materials and Methods

All equine care and investigational procedures were performed at Cornell University according to Institutional Animal Care and Use Committee-approved protocols. Horse sternal BMA was collected in the operating room from 8 young adult horses (3 castrated male and 5 female, 2 to 4 years of age). A 60-mL aliquot of BMA from each horse was processed using SmartPrep 2 BMAC (Harvest Technologies) according to the manufacturer's protocol. One horse was lost to follow-up for reasons unrelated to the study. The repair tissues from the remaining 7 horses were analyzed by arthroscopic, magnetic resonance imaging (MRI), and histological assessments 1 year after surgery.

Equine Chondral Defect and Repair Models

Full-thickness, critical-sized[28] chondral defects were created arthroscopically in the midlateral trochlear ridge of bilateral stifles by experienced equine surgeons (L.A.F., T.M.M.) using a 15-mm-diameter cutter according to a previously described technique[23]. Calcified cartilage was removed with a curette. After defect creation, 1 limb of each animal was randomly assigned to receive microfracture treatment using a standard microfracture awl to puncture the subchondral plate within the lesion bed in a standardized pattern. The contralateral limbs were switched to CO_2 for joint distension, after which the chondral lesions were dried. BMC mixed 10:1 with bovine thrombin and calcium chloride to form a clot was then arthroscopically applied directly into the dried defect. CO_2 arthroscopy was maintained until clotting was observed. Full joint range of motion was then tested to visually verify BMC clot stability within the defect.

The horses were returned to free stall activity immediately after surgery. An incremental walking program was initiated 2 weeks after surgery. Free pasture exercise was permitted 3.5

TABLE I The Bern Score for Evaluation of Chondrogenesis[31]

Scoring Category	Score*
Uniformity and darkness† of Safranin O-fast green stain	
No stain	0
Weak staining of poorly formed matrix	1
Moderately even staining	2
Even dark stain	3
Distance between cells/amount of matrix accumulated	
High cell densities with no matrix in between (no spacing between cells)	0
High cell densities with little matrix in between (cells <1 cell size apart)	1
Moderate cell density with matrix (cells approx. 1 cell size apart)	2
Low cell density with moderate distance between cells (>1 cell size) and an extensive matrix	3
Cell morphologies represented	
Condensed/necrotic/pyknotic bodies	0
Spindle/fibrous	1
Mixed spindle/fibrous with rounded chondrogenic morphology	2
Majority rounded/chondrogenic	3

*Minimum score = 0, and maximum score = 9. †Section 3 to 4 mm thick.

TABLE II Morphological MRI Assessment Grading Scheme

Grading Category	Grade
Repair fill %	
67-100	1
34-66	2
0-33	3
Bone overgrowth	
None to mild	1
Moderate	2
Severe	3
Sclerosis	
None to mild	1
Moderate	2
Severe	3
Synovial reaction	
No	0
Yes	3

months after surgery, until study completion. Gait examinations made prior to surgery and before euthanasia showed no gait asymmetries at either time point.

In Vitro Assessments

Samples of BMA, BMC, and Ficoll gradient isolates of BMA from 7 horses were evaluated. From each sample, 300,000 cells/cm^2 were plated on standard tissue culture plates in growth media[29]. Total cell counts were obtained at first passage after 14 days of culture. The chondrogenic potential of freshly isolated and culture-expanded cells was tested using a previously described 3-dimensional (3-D) pellet culture assay[30] for evaluating pellet formation after transforming growth factor-beta 1 (TGF-β1) stimulation. Chondrogenesis was assessed by pellet area, safranin O-fast green staining, and histological grading with the Bern score[30,31]. The Bern score (Table I) evaluates the uniformity and intensity of safranin O stain; the distance between cells, reflecting the amount of matrix; and cell morphology[31]. Monolayer cultures of cells from the BMA, BMC, and Ficoll groups were tested for osteogenesis by alizarin red staining and for adipogenesis, by oil red O staining.

Arthroscopic Evaluation

Cartilage repairs were arthroscopically assessed and video recorded at the 1-year follow-up by an experienced orthopaedic surgeon blinded to the treatment group (C.R.C.). Two experienced surgeons (C.R.C. and L.A.F.) graded the de-identified videos using the International Cartilage Repair Society (ICRS) macroscopic evaluation scoring system (scale of 0 to 12, where 12 is normal)[32]. The repairs were independently scored by the 2 blinded graders, who then derived consensus scores for the percent of defect repair, integration into the border zone, macroscopic appearance, and overall assessment.

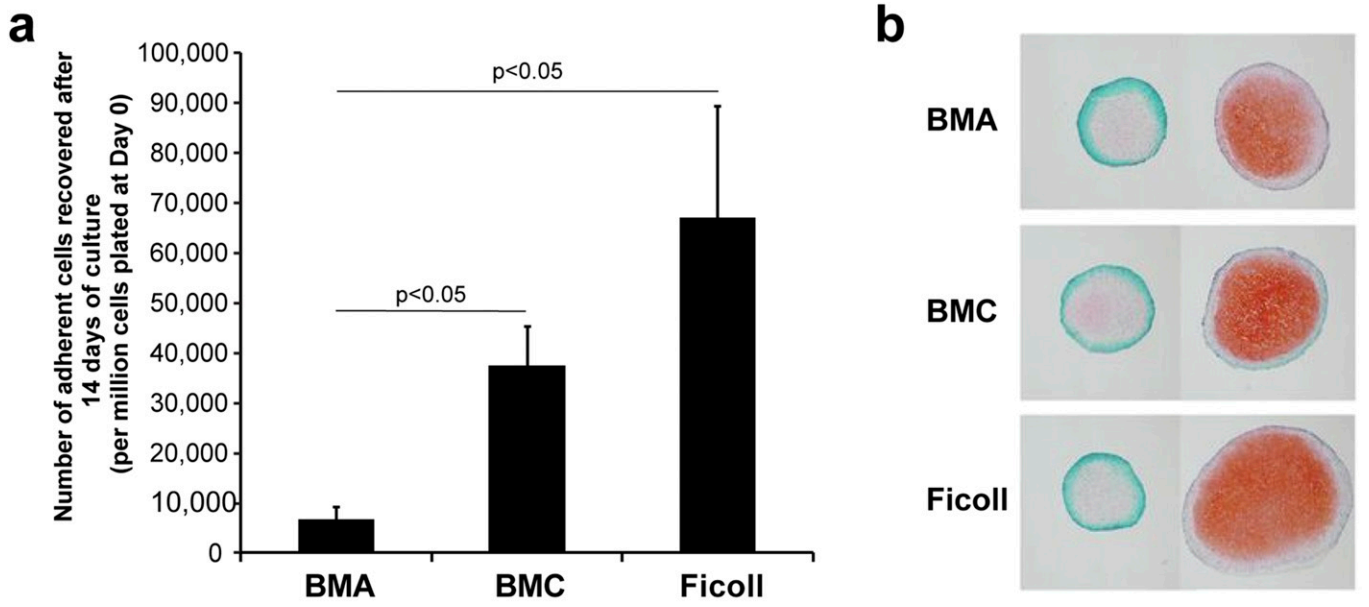

Fig. 1

Fig. 1-A Both bone marrow concentrate (BMC) and Ficoll gradient isolated cell preparations yielded a greater mean number of adherent cells compared with bone marrow aspirate (BMA) ($p < 0.05$) after 14 days of culture (I bars indicate the standard error of the mean). There were 5.5 times more adherent cells recovered from BMC than from BMA ($p = 0.005$). **Fig. 1-B** Adherent cells from all 3 preparations showed trilineage potential consistent with mesenchymal stem cells. Safranin O-fast green staining of pellets cultured in media supplemented with TGF-β1 (right column) show successful chondrogenesis from mesenchymal stem cells derived from BMA, BMC, and Ficoll isolation compared with unstimulated control pellets from each preparation (left column).

Morphological MRI

Intact stifles underwent 3-T MRI evaluations using a 3-D double-echo steady-state (DESS; Siemens Medical Solutions) sequence with water excitation and with settings as follows: 14-cm field of view, 0.7-mm slice thickness, in-plane resolution of 437 × 437 μm, and TR (repetition time) and TE (echo time) of 16.4 and 4.9 ms. The DESS images were graded on the basis of repair tissue fill, subchondral bone overgrowth, subchondral sclerosis, and synovial reaction[23] by a musculoskeletal radiologist (D.J.) who was blinded to the treatment groups (Table II). Synovial reaction was assessed as the area of high signal intensity in the soft tissues adjacent to the cartilage judged to be focal synovitis by the experienced radiologist (D.J.).

Quantitative MRI

The explanted lateral trochlear ridge was mounted on an acrylic registration plate for axial T2-weighted and ultrashort echo time enhanced T2* (UTE-T2*) MRI mapping using a 3-T MRI scanner (Siemens Medical Solutions) with an 8-channel knee coil (Invivo). Axial T2-weighted images were acquired using a multi-echo, multi-slice spin-echo sequence with 7 echoes (TE = 11, 22, 33, 44, 55, 66, and 77 ms) and with a TR of 1,800 ms, in-plane resolution of 313 × 313 μm, and 2-mm slice thickness. Axial 3-D acquisition-weighted stack of spirals (AWSOS) images[33-35] were acquired at 10 echo times (TE = 0.6, 1, 2, 3, 4, 5, 7, 10, 20, and 28 ms) and with in-plane resolution of 234 × 234 μm and 2-mm slice thickness.

T2 and UTE-T2* MRI maps were calculated from an axial slice through the center of the repair. A region of interest was manually drawn on each fitted map to encompass the full-thickness depth and width of the cartilage repair. Mean T2 and UTE-T2* values were recorded for each region of interest.

Cartilage matrix organization was measured on the calculated T2 and UTE-T2* maps using gray-level co-occurrence matrix (GLCM) second-order texture statistics from in-house developed software running on a MATLAB platform (MathWorks)[36,37]. Four statistical features ("contrast," "homogeneity," "correlation," and "energy"), calculated as previously reported[37],

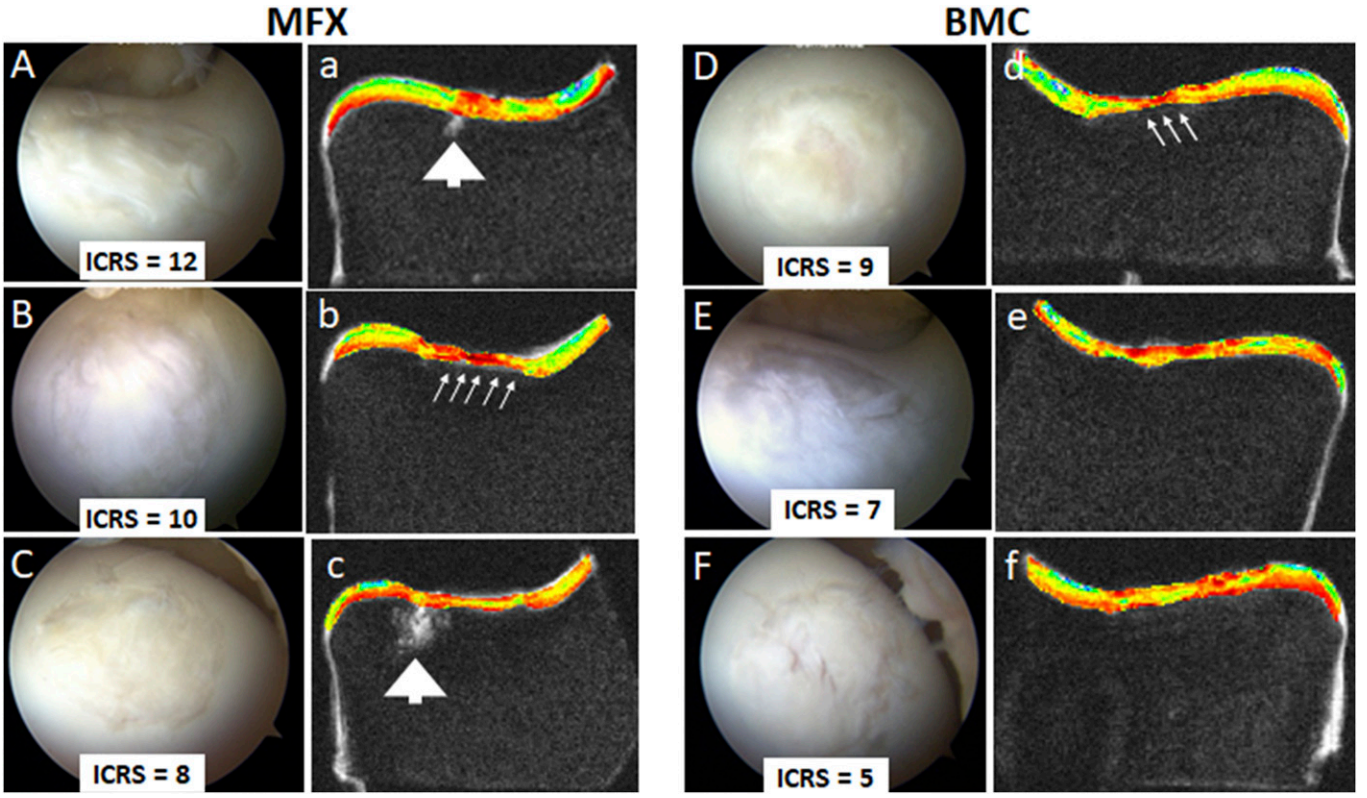

Fig. 2

Figs. 2-A through 2-f Arthroscopic and MRI evaluations show different aspects of the best 3 repairs (by arthroscopic assessment) in the 2 treatment groups: microfracture (MFX) and bone marrow concentrate (BMC). International Cartilage Repair Society (ICRS) scores are indicated. Arthroscopic evaluation provides surface imaging and tactile feedback. Images of the highest-scoring repairs in each group provide examples of improved surface characteristics observed in the microfracture group (**Figs. 2-A, 2-B, and 2-C**) compared with the BMC group (**Figs. 2-D, 2-E, and 2-F**). MRI provides cross-sectional information and shows subchondral bone voids (arrowheads) in 2 microfracture repairs (**Figs. 2-a and 2-c**), subchondral bone encroachment into the cartilage repair area (small arrows) in 1 microfracture (**Fig. 2-b**) and 1 BMC (**Fig. 2-d**) repair, and thin repair tissues in 2 microfracture repairs (**Figs. 2-b and 2-c**) and 1 BMC repair **(Fig. 2-d**). Quantitative MRI techniques such as UTE-T2* mapping (**Figs. 2-a through 2-f**) provide additional information on repair tissue subsurface matrix structure measured through texture analysis that may not be readily apparent on visual inspection.

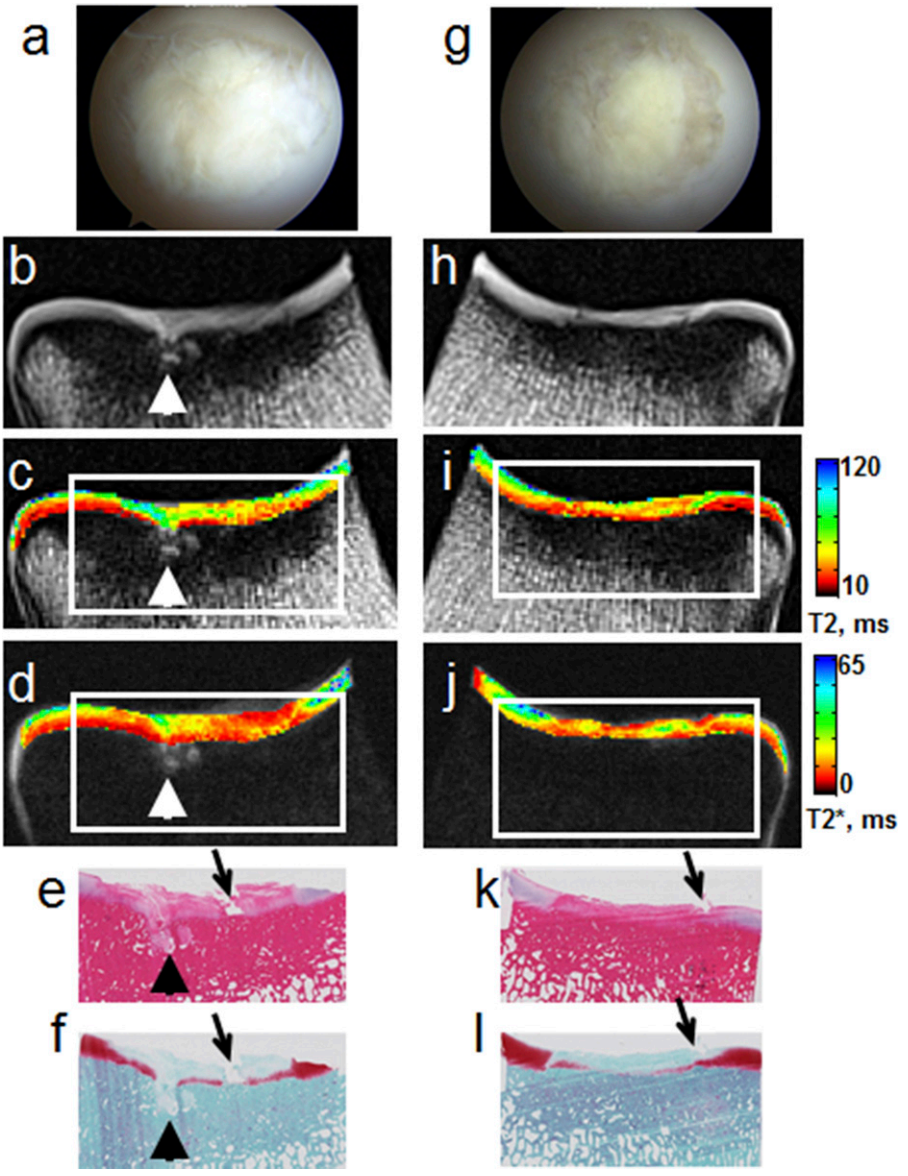

Fig. 3

Figs. 3-A through 3-L Morphological MRI evaluation shows subchondral bone changes but may not show surface defects apparent through arthroscopic and histological evaluation. Bilateral images from the same horse 1 year after treatment of full-thickness chondral defects with microfracture on 1 side (**Figs. 3-A through 3-F**) compared with bone marrow concentrate (BMC) on the contralateral side (**Figs. 3-G through 3-L**). The microfracture repair was determined to be of higher overall quality by arthroscopic surface imaging and examination (**Figs. 3-A and 3-G**). However, cross-sectional MRI and histological assessments showed compromised subchondral bone in the microfracture group (**Figs. 3-B through 3-F**). Arthroscopic (**Figs. 3-A and 3-G**) and histological evaluation (**Figs. 3-E through 3-L**) also showed surface defects (arrows) in both repairs that were not apparent on morphological MRI (**Figs. 3-B and 3-H**), likely because of partial volume effects. Images from the defect treated with microfracture (**Figs. 3-A through 3-F)** show good repair tissue fill with incomplete peripheral integration, central full-thickness fissuring, and compromised subchondral bone. Images from the defect in the contralateral limb treated with BMC (**Figs. 3-G through 3-L)** show good repair tissue fill with incomplete peripheral integration and intact subchondral bone. Morphological MRI (**Figs. 3-B and 3-H**) shows thicker repair tissue in the microfracture repair (**Fig. 3-B**). Quantitative MRI T2 maps (**Figs. 3-C and 3-I**) and UTE-T2* maps (**Figs. 3-D and 3-J**) suggest improved partial recovery of laminar patterns in the repair zones of the BMC repairs (**Figs. 3-I and 3-J**). This qualitative interpretation is reflected in the overall texture analysis of UTE-T2* maps, which showed greater "contrast," less "homogeneity," and less "energy" for BMC repairs compared with microfracture. Hematoxylin and eosin staining (**Figs. 3-E and 3-K**) demonstrates deep to full-thickness tissue voids and fissures (arrow) as well as deep-tissue heterogeneity and a bone void (arrowhead) below the repair treated with microfracture (**Fig. 3-E**). The hematoxylin and eosin staining of the BMC repair shows incomplete integration (arrow) with more intact deep tissue and no bone void (**Fig. 3-K**). Safranin O-fast green staining shows no substantial proteoglycan in the repair tissues (**Figs. 3-F and 3-L**).

were investigated at a 1-pixel offset perpendicular (90°) to the repair tissue surface.

Histological Assessment

Osteochondral slabs were fixed, decalcified, embedded in paraffin, sectioned, and stained with hematoxylin and eosin and safranin O-fast green. The de-identified stained sections were consensus-scored by 2 graders (L.A.F. and M.E.B.) according to the ICRS Visual Histological Assessment Scale (scale of 0 to 18, with 18 being normal)[38] to evaluate surface integrity, matrix structure, cell distribution, and population viability as well as subchondral bone and cartilage mineralization.

Statistical Methods

Data were examined with Shapiro-Wilk tests to assess the normality of the distributions. Nonparametric assessments were used when Shapiro-Wilk tests indicated that the assumptions of normality were violated. A Kruskal-Wallis test was used to examine differences among BMC, BMA, and Ficoll gradient samples with respect to adherent cell yield from in vitro assays, and paired t tests were used to assess differences between BMC and BMA in adherent cell yield as well as differences in morphological MRI scores and quantitative MRI values between different limbs within the same animal. Wilcoxon signed-rank tests were used to assess differences in arthroscopic and histological scores between paired limbs of the same animal from the different treatment groups.

Results

In Vitro Assays

The mean total number of nucleated cells in BMA (± standard error of the mean) was $1.92 \times 10^{11} \pm 2.64 \times 10^{10}$ and was reduced after processing into BMC ($9.66 \times 10^{9} \pm 2.37 \times 10^{9}$; $p = 0.008$ compared with BMA) or by Ficoll gradient isolation ($7.32 \times 10^{8} \pm 3.35 \times 10^{8}$; $p = 0.008$ compared with BMA). After plating and 14 days of culture, cell yields from BMC and Ficoll isolation were greater than from BMA (Kruskal-Wallis test, $p = 0.004$) (Fig. 1). After culture expansion, BMC yielded 5.5 times more cells than BMA (paired t test, $p = 0.005$).

Fresh BMA, BMC, and Ficoll gradient isolated bone marrow cells did not undergo chondrogenesis in pellet culture. Culture-expanded cells from BMA, BMC, and Ficoll gradient preparations displayed trilineage differentiation (chondrogenic, osteogenic, and adipogenic potential). With respect to chondrogenesis, pellet size increased in response to TGF-β1 in all culture-expanded cell groups, with no significant differences noted among the groups (Fig. 1). Pellets from all culture-expanded cell groups exposed to TGF-β1 demonstrated positive safranin O-fast green staining (Fig. 1) and did not differ in Bern score ($p > 0.05$).

Arthroscopic Evaluation

Repair tissue was observed throughout the defect bilaterally in 6 of the 7 horses and filled at least 50% of the defect depth in 6 of 7 of the BMC repairs and in 5 of 7 of the microfracture repairs. One horse showed a sparse 25% repair in both defects. Mean ICRS scores did not differ between the microfracture and BMC groups ($n = 7$; mean of 6.7 ± 3.6 compared with 5.4 ± 2.0, respectively; Wilcoxon signed-rank tests, $p = 0.22$). The highest and lowest arthroscopic scores were in the microfracture group, where ICRS scores ranged from 2 to 12, with higher scores indicative of a better quality of repair (Fig. 2). With respect to overall arthroscopic assessment, 3 of 7 repairs in the microfracture group were scored as "normal" to "nearly normal"; 2 of 7, "abnormal"; and 2 of 7, "severely abnormal." In the BMC group, 6 of 7 repairs were scored as "abnormal," and 1 repair, "severely abnormal."

Morphological MRI

Repair tissue was noted to have filled 67% to 100% of the defect in 2 of 7 microfracture repairs and 4 of 7 BMC repairs. Moderate to severe subchondral bone overgrowth was observed in 5 of 7 microfracture repairs and 2 of 7 BMC repairs. There was a trend toward less subchondral bone overgrowth after treatment with BMC compared with microfracture (mean grade, 1.6 ± 1.0 compared with 2.3 ± 1.0; paired t test, $p = 0.09$). Moderate to severe sclerosis was observed in 3 of 7 microfracture repairs and 1 of 7 BMC repairs. Synovial reaction was observed in 6 of 7 microfracture repairs and 4 of 7 BMC repairs. Synovial reaction was confined to the area of implantation, except in 1 microfracture case, which also showed synovitis cephalad to the repair site. The microfracture group showed worse overall MRI scores than did the BMC group (8.4 ± 1.8 compared with 6.3 ± 3.6; paired t test, $p = 0.027$), where higher scores reflect inferior joint outcomes (Table II).

Quantitative MRI

T2 (Fig. 3) and UTE-T2* MRI maps (Figs. 2 and 3) showed heterogeneous repair tissue patterns. Mean T2 and UTE-T2* values did not differ between the microfracture and BMC-treated

TABLE III Quantitative MRI: GLCM Texture Statistics by Treatment†

	MFX‡	BMC‡	P Value§
T2			
Contrast	2.61 ± 0.56	2.66 ± 0.64	0.87
Homogeneity	0.59 ± 0.04	0.58 ± 0.04	0.51
Energy	0.06 ± 0.02	0.07 ± 0.03	0.71
Correlation	0.44 ± 0.11	0.32 ± 0.17	0.31
UTE-T2*			
Contrast	0.80 ± 0.26	1.16 ± 0.25	0.03#
Homogeneity	0.75 ± 0.03	0.69 ± 0.03	0.01#
Energy	0.14 ± 0.04	0.09 ± 0.03	0.04#
Correlation	0.67 ± 0.12	0.58 ± 0.08	0.20

†GLCM= gray-level co-occurrence matrix. "Contrast" measures the amount of local T2 variation, "homogeneity" measures the T2 similarities between voxels and their neighbors, "correlation" measures linear dependencies of T2 values, and "energy" measures the orderliness of the T2 distribution[36]. ‡The values are given as the mean and the standard deviation. MFX = microfracture, and BMC = bone marrow concentrate. §Paired t test. #Significant.

repairs. No differences were observed in T2 texture statistics between microfracture and BMC ($p \geq 0.31$) (Table III). However, UTE-T2* texture statistics showed that BMC repairs had significantly greater contrast ($p = 0.03$), less homogeneity ($p = 0.01$), and less energy ($p = 0.04$) than microfracture repairs (Table III).

Histological Assessment

Both the microfracture and BMC repairs showed fibrous to fibrocartilaginous tissues. Safranin O-fast green staining was qualitatively diminished in all repairs (Fig. 3). No differences in ICRS histological scores were detected between the treatment groups for any individual criterion or total scores (Wilcoxon signed-rank tests, $p > 0.17$).

Discussion

This study demonstrated that arthroscopic application of minimally manipulated autologous BMC directly to large, full-thickness chondral defects in an equine model resulted in repairs with fibrous to fibrocartilaginous tissues similar to those observed in microfractured defects at 1 year of follow-up. The in vitro data also showed that neither BMC nor BMA, which was tested as a surrogate for microfracture, contain notable amounts of mesenchymal stem cells. While the repair tissues within the cartilage defect appeared similar between groups, MRI assessment, in which the subchondral bone and synovium were also evaluated, showed better outcomes for the BMC group, suggesting a potential positive effect of reduced surgical trauma to the subchondral bone.

An important finding of this study was that neither cells from BMA nor cells from BMC prepared using a standard clinical system at the point of care underwent chondrogenesis in pellet culture. Neither BMA, tested as a surrogate for what can optimally be obtained from microfracture, nor BMC meet minimal criteria for characterization as mesenchymal stem cells (MSC). As defined by the International Society for Cellular Therapy (ISCT), "First, MSC must be plastic-adherent when maintained in standard culture conditions."[39] The remaining 2 minimal criteria describe specific surface molecules and the ability to differentiate into osteoblasts, adipocytes, and chondroblasts in vitro[39]. While few consider microfracture a stem-cell therapy, this outcome for BMC highlights the paucity of mesenchymal stem cells in minimally manipulated preparations that are not culture-expanded.

The data did show that, after culture expansion, BMC yielded higher concentrations of mesenchymal stem cells than did BMA. Culture-expanded cells from both BMA and BMC showed appropriate equine cell surface markers[23] and displayed trilineage potential, thereby meeting the ISCT criteria for mesenchymal stem cells. This study also showed that the plastic-adherent cells from both BMA and BMC had chondrogenic potential similar to that of adherent cells from traditional Ficoll gradient isolates. Taken together, our data suggest that BMC has a higher concentration of mesenchymal stem cells than unprocessed bone marrow accessible by marrow stimulation.

The current study protocol and outcomes differ from those of a previous equine study in which BMC augmentation of chondral defects treated with microfracture improved repair tissue quality compared with microfracture alone[23]. This prior positive outcome of BMC treatment suggests that other mechanisms in addition to the few mesenchymal stem cells in BMC, such as paracrine, anti-inflammatory, or immunomodulatory effects, may be responsible for tissue regeneration. Proteomic investigations of BMC have shown substantially increased levels of interleukin 1 receptor antagonist protein (IRAP)[40], an anti-inflammatory mediator showing potential chondroprotective effects[41]. These potential effects of BMC and/or the presence of a hyaluronic acid scaffold may have also contributed to the results of a previous study in which BMC in a hyaluronic acid-based scaffold showed improved medium-term outcomes compared with microfracture in humans[27]. Further research into BMC mechanisms is needed.

Although the small numbers in this hypothesis-generating equine study substantially limit the generalizability of our findings, the comprehensive multidisciplinary assessments illustrate several important points applicable to human clinical study. First, the data provide information on the relative utility of arthroscopy, MRI, and quantitative MRI for evaluating the repair of large chondral defects that approach the size of clinically relevant lesions in humans. Each modality can be used to measure structural outcomes in a different fashion and on a different scale. Histological evaluation is destructive, severely limited in scope, and not clinically feasible. It did, however, provide detailed confirmatory information for small regions of interest. Macroscopic assessments by arthroscopy primarily showed the cartilage repair, and thus subchondral bone changes observable by MRI and histological evaluation were not well seen by arthroscopy. On the other hand, repair tissue surface fissuring that was detectable by arthroscopic and histological evaluation was not well visualized by MRI because of limitations imposed by slice thickness and partial volume effects (Fig. 3).

Nevertheless, morphological and quantitative MRI offer several advantages for human clinical evaluation of cartilage repair. Being noninvasive and nondestructive, MRI can be readily employed for human clinical evaluations and for longitudinal studies. Quantitative MRI provides additional information on repair tissue matrix organization. The UTE-T2* metric is particularly sensitive to cartilage deep-tissue structure[42]. Differences in UTE-T2* GLCM texture statistics related to contrast, homogeneity, and energy suggestive of a more developed laminar structure parallel to the bone/repair interface in BMC-treated repairs may therefore reflect improved repair tissue organization related to reduced surgical trauma. This interpretation is supported by the findings of a study by Welsch et al., wherein matrix-associated autologous chondrocyte transplantation (MACT) showed zonal variations in T2 values while microfracture repairs did not[43].

The arthroscopic appearance of the repairs also provides insight into variable human clinical outcomes after microfracture[9,15,17,19,22,44]. By arthroscopic evaluation, repairs with both

the best and the worst appearance were in the microfracture group. If similar variability of this 1-year appearance among horses occurred in humans, the data suggest that some would likely do very well in early clinical follow-up while others would experience limited to no benefit.

The durability of the repair, however, may be affected by subchondral bone changes. While the sample size was small, morphological MRI in the present study showed outcomes suggestive of improved subchondral bone characteristics in the BMC repairs compared with the microfracture repairs. These data support continued efforts to minimize bone injury from marrow-stimulation procedures through the use of narrower awls or small-diameter drills[21,45] or by the development of alternative treatment strategies.

In summary, this study showed that arthroscopic application of BMC to critical-sized chondral defects in an equine model resulted in fibrous to fibrocartilaginous repairs similar to repair by microfracture. While BMC treatment did not yield hyaline cartilage, MRI outcomes suggest less damage to the subchondral bone, potentially from reduced surgical trauma. The data also showed that there were not enough mesenchymal stem cells in minimally manipulated BMC to generate cartilaginous pellets in vitro. Thus, the finding of fibrous to fibrocartilaginous repairs observed in this study following BMC treatment should not be extrapolated to mean that mesenchymal stem cell therapies lack chondrogenic effect. Nevertheless, these results highlight the continued paucity of good options where no technology has yet convincingly replaced microfracture as a clinical standard. The continued development of strategies to promote in vivo chondroprogenitor cell differentiation remains critically important for advancing the clinical treatment of large, full-thickness chondral defects. ■

NOTE: The authors gratefully acknowledge the contributions of Stephen Bruno, Albert Chen, Christian Coyle, Jenny Erhart, Amgad Haleem, Veronica Liu, Yongxian Qian, Robert Sah, and Kimberly Sutter.

Constance R. Chu, MD[1,2]
Lisa A. Fortier, DVM, PhD[3]
Ashley Williams, MS[1]
Karin A. Payne, PhD[4]
Taralyn M. McCarrel, DVM[5]
Megan E. Bowers, PhD[6]
Diego Jaramillo, MD, MPH[2,7]

[1]Department of Orthopedic Surgery, Stanford University, Stanford, California

[2]VA Palo Alto Health Care System, Palo Alto, California

[3]College of Veterinary Medicine, Cornell University, Ithaca, New York

[4]Department of Orthopedics, University of Colorado, Aurora, Colorado

[5]College of Veterinary Medicine, University of Florida, Gainesville, Florida

[6]George Washington University, Washington, DC

[7]Nicklaus Children's Hospital, Miami, Florida

E-mail address for C.R. Chu: chucr@stanford.edu

ORCID iD for C.R. Chu: 0000-0002-4998-5846

References

1. Martin JA, Brown T, Heiner A, Buckwalter JA. Post-traumatic osteoarthritis: the role of accelerated chondrocyte senescence. Biorheology. 2004;41(3-4):479-91.
2. Squires GR, Okouneff S, Ionescu M, Poole AR. The pathobiology of focal lesion development in aging human articular cartilage and molecular matrix changes characteristic of osteoarthritis. Arthritis Rheum. 2003 May;48(5):1261-70. Epub 2003 May 15.
3. Widuchowski W, Widuchowski J, Trzaska T. Articular cartilage defects: study of 25,124 knee arthroscopies. Knee. 2007 Jun;14(3):177-82. Epub 2007 Apr 10.
4. Dillon CF, Rasch EK, Gu Q, Hirsch R. Prevalence of knee osteoarthritis in the United States: arthritis data from the Third National Health and Nutrition Examination Survey 1991-94. J Rheumatol. 2006 Nov;33(11):2271-9. Epub 2006 Oct 1.
5. Lawrence RC, Felson DT, Helmick CG, Arnold LM, Choi H, Deyo RA, Gabriel S, Hirsch R, Hochberg MC, Hunder GG, Jordan JM, Katz JN, Kremers HM, Wolfe F; National Arthritis Data Workgroup. Estimates of the prevalence of arthritis and other rheumatic conditions in the United States. Part II. Arthritis Rheum. 2008 Jan;58(1):26-35. Epub 2008 Jan 1.
6. Mankin HJ. The response of articular cartilage to mechanical injury. J Bone Joint Surg Am. 1982 Mar;64(3):460-6.
7. Shapiro F, Koide S, Glimcher MJ. Cell origin and differentiation in the repair of full-thickness defects of articular cartilage. J Bone Joint Surg Am. 1993 Apr;75(4):532-53.
8. Frisbie DD, Trotter GW, Powers BE, Rodkey WG, Steadman JR, Howard RD, Park RD, McIlwraith CW. Arthroscopic subchondral bone plate microfracture technique augments healing of large chondral defects in the radial carpal bone and medial femoral condyle of horses. Vet Surg. 1999 Jul-Aug;28(4):242-55.
9. Steadman JR, Rodkey WG, Rodrigo JJ. Microfracture: surgical technique and rehabilitation to treat chondral defects. Clin Orthop Relat Res. 2001 Oct;391(Suppl):S362-9.
10. Magnussen RA, Dunn WR, Carey JL, Spindler KP. Treatment of focal articular cartilage defects in the knee: a systematic review. Clin Orthop Relat Res. 2008 Apr;466(4):952-62. Epub 2008 Jan 12.
11. Zaslav K, Cole B, Brewster R, DeBerardino T, Farr J, Fowler P, Nissen C; STAR Study Principal Investigators. A prospective study of autologous chondrocyte implantation in patients with failed prior treatment for articular cartilage defect of the knee: results of the Study of the Treatment of Articular Repair (STAR) clinical trial. Am J Sports Med. 2009 Jan;37(1):42-55. Epub 2008 Oct 16.
12. Bae DK, Yoon KH, Song SJ. Cartilage healing after microfracture in osteoarthritic knees. Arthroscopy. 2006 Apr;22(4):367-74.
13. Kreuz PC, Erggelet C, Steinwachs MR, Krause SJ, Lahm A, Niemeyer P, Ghanem N, Uhl M, Südkamp N. Is microfracture of chondral defects in the knee associated with different results in patients aged 40 years or younger? Arthroscopy. 2006 Nov;22(11):1180-6.
14. Kreuz PC, Steinwachs MR, Erggelet C, Krause SJ, Konrad G, Uhl M, Südkamp N. Results after microfracture of full-thickness chondral defects in different compartments in the knee. Osteoarthritis Cartilage. 2006 Nov;14(11):1119-25. Epub 2006 Jul 11.
15. Mithoefer K, Williams RJ 3rd, Warren RF, Potter HG, Spock CR, Jones EC, Wickiewicz TL, Marx RG. The microfracture technique for the treatment of articular cartilage lesions in the knee. A prospective cohort study. J Bone Joint Surg Am. 2005 Sep;87(9):1911-20.
16. Cerynik DL, Lewullis GE, Joves BC, Palmer MP, Tom JA. Outcomes of microfracture in professional basketball players. Knee Surg Sports Traumatol Arthrosc. 2009 Sep;17(9):1135-9. Epub 2009 Mar 19.
17. Gobbi A, Karnatzikos G, Kumar A. Long-term results after microfracture treatment for full-thickness knee chondral lesions in athletes. Knee Surg Sports Traumatol Arthrosc. 2014 Sep;22(9):1986-96. Epub 2013 Sep 20.
18. Mithoefer K, Williams RJ 3rd, Warren RF, Wickiewicz TL, Marx RG. High-impact athletics after knee articular cartilage repair: a prospective evaluation of the microfracture technique. Am J Sports Med. 2006 Sep;34(9):1413-8. Epub 2006 May 30.
19. Steadman JR, Miller BS, Karas SG, Schlegel TF, Briggs KK, Hawkins RJ. The microfracture technique in the treatment of full-thickness chondral lesions of the knee in National Football League players. J Knee Surg. 2003 Apr;16(2):83-6.

20. Minas T, Gomoll AH, Rosenberger R, Royce RO, Bryant T. Increased failure rate of autologous chondrocyte implantation after previous treatment with marrow stimulation techniques. Am J Sports Med. 2009 May;37(5):902-8. Epub 2009 Mar 4.

21. Madry H, Orth P, Cucchiarini M. Role of the subchondral bone in articular cartilage degeneration and repair. J Am Acad Orthop Surg. 2016 Apr;24(4):e45-6.

22. Mithoefer K, Venugopal V, Manaqibwala M. Incidence, degree, and clinical effect of subchondral bone overgrowth after microfracture in the knee. Am J Sports Med. 2016 Aug;44(8):2057-63. Epub 2016 May 17.

23. Fortier LA, Potter HG, Rickey EJ, Schnabel LV, Foo LF, Chong LR, Stokol T, Cheetham J, Nixon AJ. Concentrated bone marrow aspirate improves full-thickness cartilage repair compared with microfracture in the equine model. J Bone Joint Surg Am. 2010 Aug 18;92(10):1927-37.

24. Wilke MM, Nydam DV, Nixon AJ. Enhanced early chondrogenesis in articular defects following arthroscopic mesenchymal stem cell implantation in an equine model. J Orthop Res. 2007 Jul;25(7):913-25.

25. Gobbi A, Karnatzikos G, Sankineani SR. One-step surgery with multipotent stem cells for the treatment of large full-thickness chondral defects of the knee. Am J Sports Med. 2014 Mar;42(3):648-57. Epub 2014 Jan 23.

26. Gobbi A, Karnatzikos G, Scotti C, Mahajan V, Mazzucco L, Grigolo B. One-step cartilage repair with bone marrow aspirate concentrated cells and collagen matrix in full-thickness knee cartilage lesions: results at 2-year follow-up. Cartilage. 2011 Jul;2(3):286-99.

27. Gobbi A, Whyte GP. One-stage cartilage repair using a hyaluronic acid-based scaffold with activated bone marrow-derived mesenchymal stem cells compared with microfracture: 5-year follow-up. Am J Sports Med. 2016 Nov;44(11):2846-54. Epub 2016 Jul 29.

28. Sams AE, Minor RR, Wootton JA, Mohammed H, Nixon AJ. Local and remote matrix responses to chondrocyte-laden collagen scaffold implantation in extensive articular cartilage defects. Osteoarthritis Cartilage. 1995 Mar;3(1):61-70.

29. Radcliffe CH, Flaminio MJ, Fortier LA. Temporal analysis of equine bone marrow aspirate during establishment of putative mesenchymal progenitor cell populations. Stem Cells Dev. 2010 Feb;19(2):269-82.

30. Payne KA, Didiano DM, Chu CR. Donor sex and age influence the chondrogenic potential of human femoral bone marrow stem cells. Osteoarthritis Cartilage. 2010 May;18(5):705-13. Epub 2010 Feb 6.

31. Grogan SP, Barbero A, Winkelmann V, Rieser F, Fitzsimmons JS, O'Driscoll S, Martin I, Mainil-Varlet P. Visual histological grading system for the evaluation of in vitro-generated neocartilage. Tissue Eng. 2006 Aug;12(8):2141-9.

32. Brittberg M, Winalski CS. Evaluation of cartilage injuries and repair. J Bone Joint Surg Am. 2003;85(Suppl 2):58-69. Epub 2003 May 2.

33. Qian Y, Boada FE. Acquisition-weighted stack of spirals for fast high-resolution three-dimensional ultra-short echo time MR imaging. Magn Reson Med. 2008 Jul;60 (1):135-45. Epub 2008 Jun 27.

34. Williams A, Qian Y, Chu CR. UTE-T2* mapping of human articular cartilage in vivo: a repeatability assessment. Osteoarthritis Cartilage. 2011 Jan;19(1):84-8. Epub 2010 Oct 28.

35. Chu CR, Williams AA, West RV, Qian Y, Fu FH, Do BH, Bruno S. Quantitative magnetic resonance imaging UTE-T2* mapping of cartilage and meniscus healing after anatomic anterior cruciate ligament reconstruction. Am J Sports Med. 2014 Aug;42(8):1847-56. Epub 2014 May 8.

36. Haralick RM, Shanmugam K, Dinstein I. Texture features for image classification. IEEE Transactions on Systems, Man, and Cybernetics. 1973 Nov;SMC-3(6):610-21.

37. Williams A, Winalski CS, Chu CR. Early articular cartilage MRI T2 changes after anterior cruciate ligament reconstruction correlate with later changes in T2 and cartilage thickness. J Orthop Res. 2017 Mar;35(3):699-706. Epub 2016 Jul 29.

38. Mainil-Varlet P, Aigner T, Brittberg M, Bullough P, Hollander A, Hunziker E, Kandel R, Nehrer S, Pritzker K, Roberts S, Stauffer E; International Cartilage Repair Society. Histological assessment of cartilage repair: a report by the Histology Endpoint Committee of the International Cartilage Repair Society (ICRS). J Bone Joint Surg Am. 2003;85(Suppl 2):45-57.

39. Dominici M, Le Blanc K, Mueller I, Slaper-Cortenbach I, Marini F, Krause D, Deans R, Keating A, Prockop Dj, Horwitz E. Minimal criteria for defining multipotent mesenchymal stromal cells. The International Society for Cellular Therapy position statement. Cytotherapy. 2006;8(4):315-7.

40. Cassano JM, Kennedy JG, Ross KA, Fraser EJ, Goodale MB, Fortier LA. Bone marrow concentrate and platelet-rich plasma differ in cell distribution and interleukin 1 receptor antagonist protein concentration. Knee Surg Sports Traumatol Arthrosc. 2016 Feb 1. [Epub ahead of print].

41. Frisbie DD, Bowman SM, Colhoun HA, DiCarlo EF, Kawcak CE, McIlwraith CW. Evaluation of autologous chondrocyte transplantation via a collagen membrane in equine articular defects: results at 12 and 18 months. Osteoarthritis Cartilage. 2008 Jun;16(6):667-79. Epub 2007 Nov 26.

42. Du J, Carl M, Bae WC, Statum S, Chang EY, Bydder GM, Chung CB. Dual inversion recovery ultrashort echo time (DIR-UTE) imaging and quantification of the zone of calcified cartilage (ZCC). Osteoarthritis Cartilage. 2013 Jan;21(1):77-85. Epub 2012 Sep 28.

43. Welsch GH, Mamisch TC, Domayer SE, Dorotka R, Kutscha-Lissberg F, Marlovits S, White LM, Trattnig S. Cartilage T2 assessment at 3-T MR imaging: in vivo differentiation of normal hyaline cartilage from reparative tissue after two cartilage repair procedures—initial experience. Radiology. 2008 Apr;247(1):154-61. Epub 2008 Mar 29.

44. Steadman JR, Briggs KK, Rodrigo JJ, Kocher MS, Gill TJ, Rodkey WG. Outcomes of microfracture for traumatic chondral defects of the knee: average 11-year follow-up. Arthroscopy. 2003 May-Jun;19(5):477-84.

45. Chen H, Sun J, Hoemann CD, Lascau-Coman V, Ouyang W, McKee MD, Shive MS, Buschmann MD. Drilling and microfracture lead to different bone structure and necrosis during bone-marrow stimulation for cartilage repair. J Orthop Res. 2009 Nov;27(11):1432-8.